

Processing and electrical conductivity of lanthanum gallate core-shell heterostructures

E. GOMES^{A,B}, F.M. FIGUEIREDO^{A,C}, F.M.B. MARQUES^A

^aDep. of Ceramics and Glass Eng., CICECO, University of Aveiro, P3810-193 Aveiro.

^bESTG, Instituto Politécnico de Viana do Castelo, P4900-348 Viana do Castelo.

^cSci. and Tech. Dep., Universidade Aberta, R. Escola Politécnica 147, P1269-001 Lisbon.

The electrical properties of a lanthanum gallate solid electrolyte were modified by selectively doping the grain boundaries with Fe. This was achieved by sandwiching a $\text{La}_{0.95}\text{Sr}_{0.05}\text{Ga}_{0.90}\text{Mg}_{0.10}\text{O}_{3-\delta}$ (LSGM) dense pellet between LaFeO_3 samples. Annealing at 1550°C in air for several hours promoted Fe diffusion into LSGM via the grain boundaries. Scanning electron microscopy and energy-dispersive spectroscopy analyses showed that iron was located at the grain boundary while the grain bulk preserved the LSGM composition. Impedance spectra obtained at low temperature consist of the two usual bulk and grain boundary contributions. A significant increase in total conductivity was observed for the iron-doped samples, the effect being greater for the grain boundary contribution. The total conductivity measured for the iron-containing material revealed a slight decrease with decreasing oxygen partial pressure, suggesting the onset of p-type electronic conduction. Estimates of the p-type electronic conductivity (σ_p) were obtained by fitting the low temperature impedance spectra to a simple equivalent circuit including one parallel electronic branch. The value for σ_p in air at 300°C is 3.1×10^{-6} S/cm and the activation energy is 75.1 kJ/mol between 300 and 400°C .

Keywords: core-shell, gallate, grain boundary, mixed conductor, impedance spectroscopy.

Procesamiento y conductividad eléctrica de galato de lantano con heteroestructura de tipo core-shell.

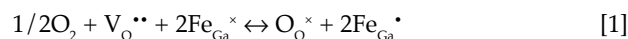
Las propiedades eléctricas de un electrolito sólido de galato de lantano se han modificado mediante un dopado eléctrico de Fe en borde de grano. Esto se consiguió preparando una estructura de sandwich con una plantilla densa de $\text{La}_{0.95}\text{Sr}_{0.05}\text{Ga}_{0.90}\text{Mg}_{0.10}\text{O}_{3-\delta}$ (LSGM) entre las muestras de LaFeO_3 . Un tratamiento de varias horas a 1550°C en aire favoreció la difusión de Fe a lo largo de los bordes de grano. Los análisis mediante microscopía electrónica de barrido y espectroscopía de energía dispersada muestran que el hierro se localiza en borde de grano mientras que se preserva la composición de LSGM en el interior de grano. En las muestras dopadas con hierro se observa un aumento de la conductividad total siendo el efecto más notable en el borde del grano. La conductividad total del material que contiene hierro presentó un ligero descenso al reducirse la presión parcial de oxígeno, lo que sugiere la presencia de conducción electrónica tipo p. La conductividad electrónica tipo (σ_p) se evaluó ajustando el espectro de impedancia de baja temperatura a un circuito equivalente sencillo con una resistencia electrónica en paralelo. El valor de σ_p en aire a 300°C es $3,1 \times 10^{-6}$ S/cm y la energía de actuación 75,1 kJ/mol entre 300 y 400°C .

Palabras clave: core-shell, galato, borde de grano, conductor mixto, espectroscopía de impedancia.

1. INTRODUCTION

The existence of mixed ionic and electronic conductivity in a material is of interest for a variety of high temperature electrochemical applications such as oxygen separation membranes. (1) The majority of most interesting materials are multicomponent oxides with the perovskite structure with the B site partly (or totally) occupied by a transition metal element, e.g.: $\text{La}_{1-x}\text{Sr}_x\text{Co}_{1-y}\text{Fe}_y\text{O}_{3-\delta}$ (2), $\text{ATi}_{1-x}\text{Fe}_x\text{O}_{3-\delta}$ ($A=\text{Ca}$, Sr) (3,4) or $\text{La}_{1-x}\text{Sr}_x\text{Ga}_{1-y}\text{Fe}_y\text{O}_{3-\delta}$ (5). The optimisation of the properties of these materials follows a traditional approach of homogeneous doping. As an example, in the case of the lanthanum gallates, $\text{La}_{1-x}\text{Sr}_x\text{Ga}_{1-y}\text{Mg}_y\text{O}_{3-\delta}$ (LSGM) is derived from LaGaO_3 by suitable doping with divalent Sr and Mg, where the resulting negative charges are compensated by formation of oxygen vacancies (6,7). Being an excellent ionic conductor, it can easily be transformed into a mixed conductor by substitution of Ga by a transition metal such as Fe (8,9). Considering this example, which one may write in abbreviated form as LSGM-Fe, it has been suggested that the conduction mechanism is linked to the hopping of small polarons between trivalent and tetravalent iron (8,9). The formation of Fe^{4+} is

favoured in oxidising conditions and may be described, using Kröger-Vink notation, by the reaction



Alternatively, mixed conducting composites may be obtained by combining an ionic conducting phase with an electronic conductor. The most common approach to these composites is a simple two-phase mixture of contiguous grains (10,11). Two-phase composites may also be designed with an alternative [core]shell structure in which one component – [core] – is surrounded by the other – shell. In the field of electroceramics, the most well known example of core-shell ceramics is that of commercial $[\text{BaTiO}_3]_{\text{core}}[\text{BaTi}_{1-x}\text{Zr}_x\text{O}_3]_{\text{shell}}$ based ferroelectric phases for temperature-stable ceramic multilayer capacitors (12); the composite benefits from a combination of the dielectric constants of both phases which have different temperature dependencies. Other applications of [core]shell structured materials include magnetic SmCo_5 particles surrounded by metallic copper (13) and semiconducting Si or

Ge cores with a shell consisting of the corresponding oxides (GeO_x and SiO_x) (14). There are no known examples of mixed electronic/ionic conductors.

Recently, the formation of metastable $[\text{CaTiO}_3]_{0.8}\text{CaTi}_{0.8}\text{Fe}_{0.2}\text{O}_{3-\delta}$ heterostructures was reported (15). Interestingly, the oxygen permeability flux (and thus the ionic conductivity) measured for the heterogeneous ceramics is considerably higher than the compositionally identical $\text{CaTi}_{0.8}\text{Fe}_{0.2}\text{O}_{3-\delta}$ homogeneous material. Since the grain boundaries in this material are resistive to oxygen transport (16), the enhancement in ionic conductivity observed for the [core]shell ceramics must be due to the new features created in the shell such as additional oxygen pathways induced by the microdomains boundaries, space charge areas adjacent to the domain and/or the core-shell boundaries. It is expected that the effect of the second phase can thus provide a new kinetic pathway, modify the structure and/or increase the defect concentrations in the zones adjacent to the boundaries.

The [core]shell design is a novel and potentially interesting approach to enhance the transport properties of mixed oxygen and electronic conductors. This work presents preliminary results describing an attempt to obtain [LSGM]LSGM-Fe [core]shell ceramics by selective Fe-impregnation of LSGM grain boundaries. The grain bulk and boundary electrical properties were studied by impedance spectroscopy and analysed using an equivalent circuit model to obtain estimates of the electronic conductivity component.

2. EXPERIMENTAL PROCEDURE

Dense samples with nominal $\text{La}_{0.95}\text{Sr}_{0.05}\text{Ga}_{0.90}\text{Mg}_{0.10}\text{O}_{3-\delta}$ (LSGM) composition were prepared via the conventional ceramic route starting from high purity lanthanum (Merck), gallium (Aldrich) and magnesium (Panreac) oxides and SrCO_3 (Merck). The La_2O_3 was previously calcined at 1100°C for 8 hours in order to decompose the small amount of $\text{La}(\text{OH})_3$ that is usually present in the original powder. The precursors were mixed in ethanol in a planetary ball mill, dried and calcined at 1100°C for 12 h and again ball-milled and dried. The resultant powder was uniaxially pressed into disk-shaped pellets and sintered at 1550°C during 4 h, with heating and cooling rates of 5 K/min. The X-ray diffraction (XRD) pattern, collected at room temperature from a powdered sample, could be indexed to the Pnma orthorhombic space group. A small amount of a secondary, unidentified phase was suggested by a very small diffraction peak. Combined scanning electron microscopy (SEM) and energy-dispersive spectroscopy (EDS) analyses confirmed the presence of a small number of Sr-enriched grains dispersed in the ceramic matrix. The grain size was found to vary in a broad range from about 5 to 15 μm . Finally, these samples have a density greater than 93% of the theoretical value (determined from XRD data).

The LSGM pellets, with both surfaces polished with 3 μm -grained diamond paste, were sandwiched between two $\text{LaFeO}_{3-\delta}$ dense pellets and annealed in air at 1550°C to presumably promote the diffusion of Fe along the LSGM grain boundaries. The pellets were submitted to various annealing cycles of 1 hour each. The heating and cooling rates were 5 K/min.

The electrical properties of the ceramic samples were studied by impedance spectroscopy in air between 300 and 500°C . The spectra were collected in the frequency range 20– 10^6 Hz with $V_{\text{ac}}=100$ mV using an Hewlett Packard 4284A

impedance analyser. Results were fitted to equivalent circuits using the dedicated code developed by Bernard Boukamp (17). Fresh platinum electrodes were applied before every measurement and gently removed before the subsequent annealing. The same analyser was used to assess the oxygen partial pressure (Po_2) dependence of the total conductivity, measured at a fixed frequency of 10 kHz. These measurements were carried out at $700\text{--}750^\circ\text{C}$ and with Po_2 varying from air down to about 10 Pa, by flowing nitrogen.

Several samples were specially prepared for SEM and EDS analyses by polishing down to 0.3 μm diamond paste and subsequent annealing at 1450°C for 30 min. Fractured, non-polished surfaces were observed aside.

3. RESULTS AND DISCUSSION

3.1. Microstructure

The SEM microstructure shown in Figure 1 was obtained for a LSGM pellet after three impregnation cycles. The grain size remains nearly unchanged by impregnation and is fairly large (in the range 10–15 μm), as usually reported for LSGM ceramics obtained by the ceramic route and sintered at temperatures higher than 1500°C (18,19). The white spots are the marks left by the electron beam during EDS analysis. Spectra collected at the centre and at the periphery of the grain (small arrows) are shown in Figure 2. They show that iron is present only at the grain periphery. The iron atomic concentration profiles, measured at the points along the two large arrows shown in Figure 1, are plotted in Figure 3, as the Fe/Ga ratio. The results suggest that the thickness of the iron containing shell varies between 1 and 2 μm . Within the fitting error (10%), the fractions of La and Ga remain unchanged, while large errors (between 50–100%) associated to the Sr and Mg fraction estimates prevent any meaningful comment on these minor lighter elements. It should be noticed that no standards were used for the EDS analyses. Therefore the data presented is semi-quantitative and hence the ratios.

Given the geometric configuration of the LSGM/ LaFeO_3 diffusion couple, an iron concentration gradient is expected to form from the surfaces to the bulk of the LSGM pellet. This was confirmed by several EDS spectra collected along the

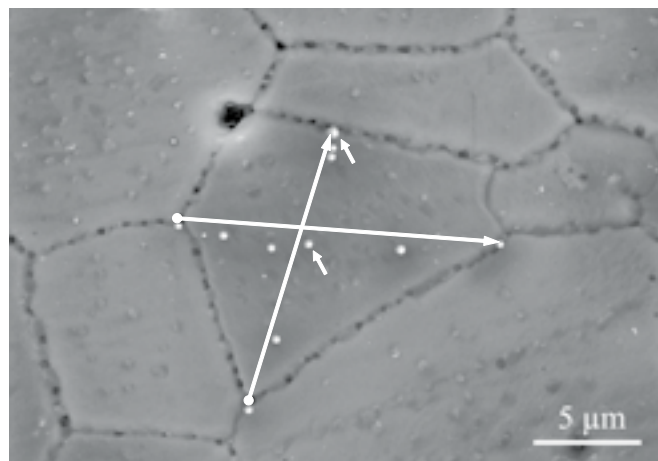


Fig. 1- SEM micrograph of one Fe-doped LSGM sample obtained after three impregnation cycles. The white spots are due to the prolonged action of the EDS.

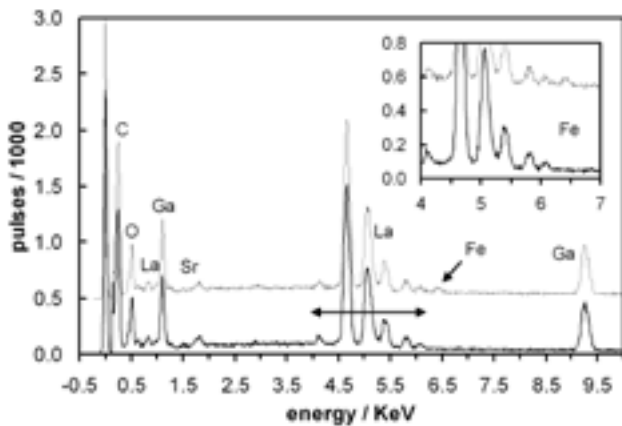


Fig. 2- EDS spectra collected at the spots indicated by the small arrows in Figure 1: bottom spectrum collected at the central spot; top spectrum collected at the periphery, with a noticeable Fe peak, also shown in the inset.

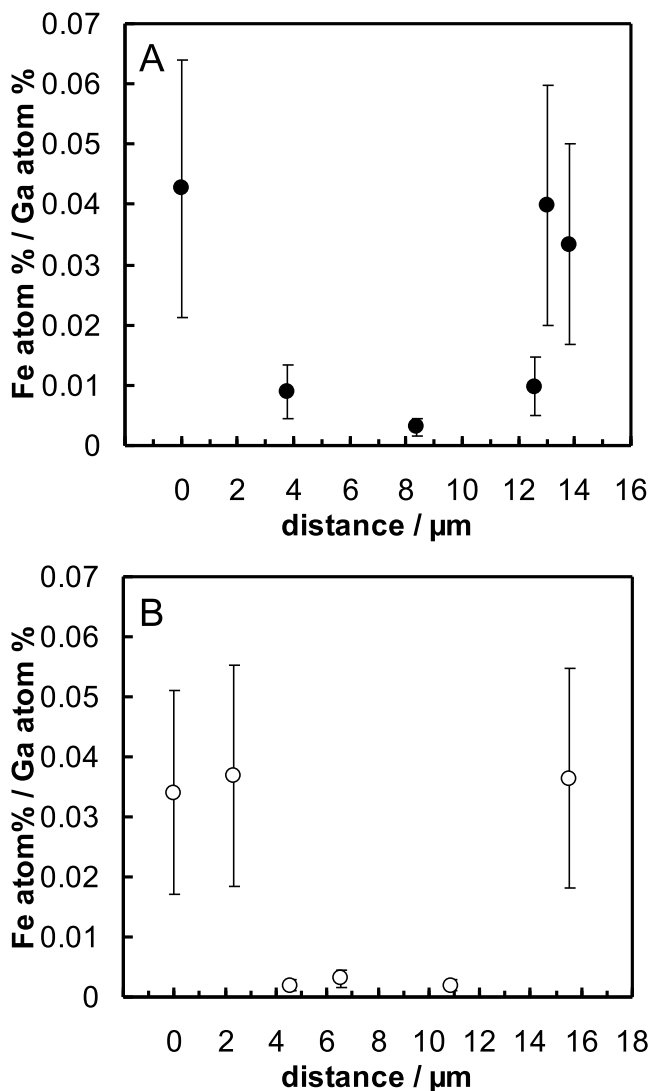


Fig. 3- Evolution of the Fe/Ga ratio along the larger white arrows in Figure 1: A) vertical, down-up; B) horizontal, left-right.

pellets cross section. Moreover, the intensity of the Fe peaks was very low (background level) in the spectra obtained at about $100 \mu\text{m}$ of each surface. Simple visual inspection showed a dark colour throughout the entire cross section of the pellets that is quite different from the light brown characteristic of Fe-free samples. This is a strong indication that the impregnation occurred in the entire pellet. The apparent disagreement with EDS may be explained by the fact that a very small number of Fe cations, acting as colour centres, should suffice to produce the optic effect. Such low amount of Fe may just have no, or a very small effect on the electrical properties.

More precise analytical techniques, such as EDS in a transmission electron microscope, with higher spatial resolution, are necessary to better characterise these ceramics. However, the preliminary results now presented confirm the formation of [LSGM]LSGM-Fe ceramics via the high temperature impregnation of dense pellets.

3.2. Impedance spectroscopy

The impedance spectra collected in air at 300°C for the fresh LSGM and impregnated [LSGM]LSGM-Fe ceramics are shown in Figure 4. The LSGM sample spectrum consists of the usual two high and low frequency contributions, which may be ascribed to the bulk and grain boundary polarisations, respectively. The spectra were thus fitted to an equivalent circuit comprising a series association of two resistors in parallel with constant phase elements (the constant phase element is preferred because the semicircles are slightly depressed). Following Boukamp's notation (17), this circuit may be represented as $(R_b Q_b)(R_{gb} Q_{gb})$, where R_i are resistors, Q_i constant phase elements and the subscripts b and gb denote bulk and grain boundary. The relevant fitting parameters are the bulk and grain boundary resistances (R_b, R_{gb}), pseudocapacitances (Q_b, Q_{gb}) and the indexes that account for the depression of the semicircles (n_b, n_{gb}). The fitting results are listed in Table 1. The true capacitance values associated to each semicircle, determined by $C = R^{(1-n)/n} Q^{1/n}$, are 16 pF and 15 nF, respectively for the high and low frequency contributions. The magnitude of these values is typical for the ionic polarisation associated to the grain and grain boundary in a polycrystalline ionic conductor. As expected from the considerably large grain size and relatively clean grain boundaries, the grain boundary contribution to the overall electrical resistance is much smaller than the grain bulk.

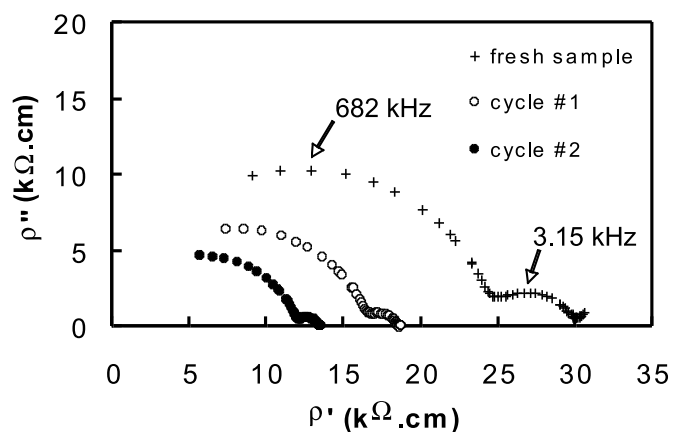


Fig. 4- Impedance spectra obtained in air at 300°C for a fresh LSGM sample and after the first and second impregnation cycles.

TABLE I. FITTING PARAMETERS OBTAINED FOR THE FRESH LSGM CERAMIC AT 300°C. ERRORS ARE GIVEN INSIDE PARENTHESIS.

Grain bulk	R_b	14857 Ω (0.2%)
	Q_b	8.6×10^{-11} (3.2%)
	n_b	0.89 (0.2%)
Grain boundary	R_{gb}	3315 Ω (1.8%)
	Q_{gb}	9.0×10^{-8} (13.2%)
	n_{gb}	0.82 (1.8%)

The effect of impregnation with iron is noticed due to the progressive decrease of the amplitude of both semicircles (R_b and R_{gb} values) as the sample is submitted to an increasing number of impregnation cycles. Moreover, the effect is greater for the grain boundary contribution. This is clearly observed in a representation of the ratio R_{gb}/R_g as a function of the number of cycles, as shown in Figure 5. Data obtained for several samples show that the trend is reproducible. This result corresponds to what is expected from the core shell microstructure of the [LSGM]LSGM-Fe ceramics (Figure 1) and strongly suggests that the overall increase in conductivity is mainly due to the appearance of a new parallel electronic pathway, resulting in the significant lowering of the grain boundary arc.

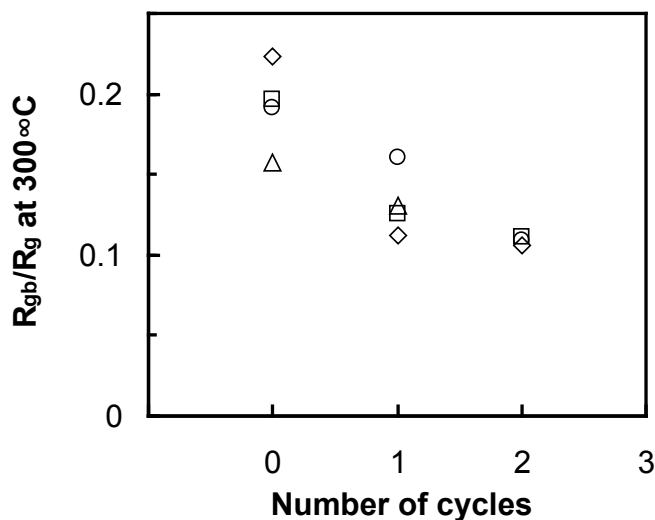


Fig. 5- Variaton of R_{gb}/R_g after subsequent impregnation cycles.

In order to confirm that the nature of the additional charge carriers is electronic, the electrical conductivity of the samples was measured as a function of P_{O_2} in moderately oxidising conditions. These results, presented in Figure 6, show that the conductivity has a slight positive tendency with increasing P_{O_2} . Although almost negligible for the fresh sample, the slope of the $\log \sigma$ versus $\log P_{O_2}$ is clearly more pronounced for the [LSGM]LSGM-Fe samples. This means that the increase in conductivity should be due to a localised increasing concentration of electron holes close to the grain boundaries, in agreement with Equation (1) or even along secondary phases, leading to an increase in the p-type electronic component of conductivity.

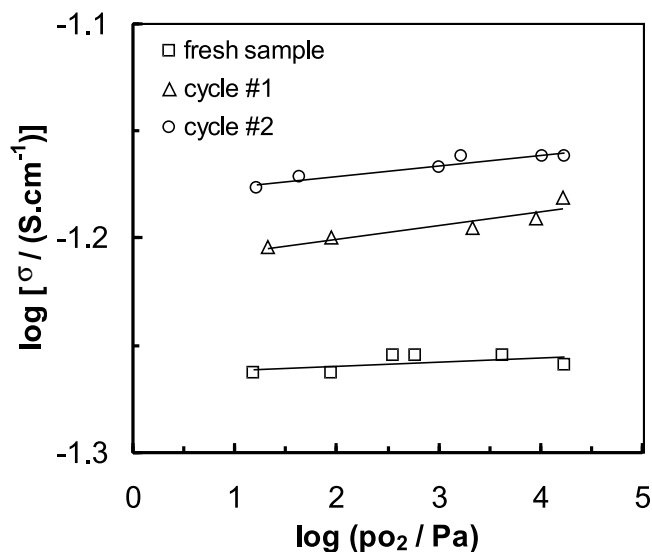


Fig. 6- Total electrical conductivity as a function of P_{O_2} at 750°C for pure LSGM and Fe-doped samples.

3.3 Model behaviour

The [LSGM]LSGM-Fe microstructure and impedance spectroscopy results configure a fairly simple model system consisting of an ionic conductor grain bulk surrounded by mixed ionic-electronic conducting grain boundaries. This can be described by adding a parallel electronic branch to the polycrystalline LSGM pure ionic conductor. The equivalent circuit model is represented in the inset in Figure 7, where the resistor R_e is the electronic resistance; the smaller R_e , the higher is the electronic conductivity. This circuit was thus used to simulate the impedance spectra of LSGM ceramics with different levels of electronic conductivity. Results are shown in Figure 7. The thicker line corresponds to the fresh sample and was obtained using the parameters listed in Table

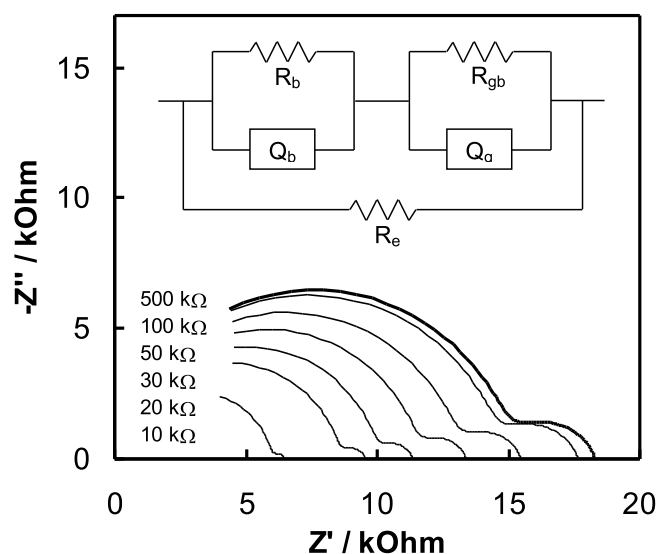


Fig. 7- Equivalent circuit and impedance spectra simulated with the parameters listed in Table 1 and R_e values of 500, 100, 50, 30, 20 and 10 k Ω .

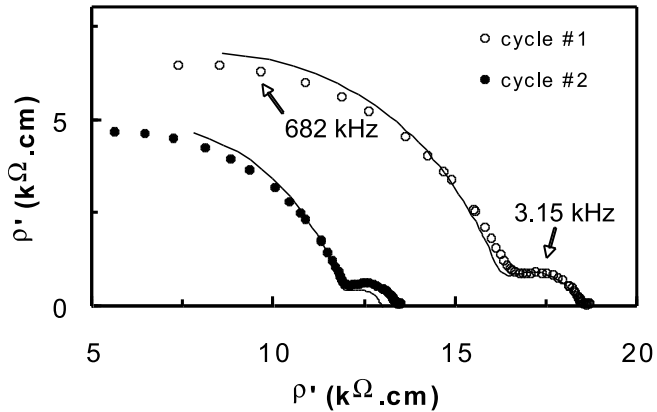


Fig. 8- Impedance spectra of LSGM after two Fe impregnation cycles and the corresponding fits to the equivalent circuit described in Figure 7. The best fit is obtained, for the first cycle, with $R_e=28878$ and 13836 Ω for the second.

1 and a circuit comprising only the two (RQ) components. The thinner lines show the modified spectra as R_e is decreased – or electronic conductivity is increased. The similarities with the experimental results (Figure 4) are obvious. Thus, the model was used to fit the spectra of the impregnated samples in order to obtain estimates of R_e while keeping the other parameters fixed and set equal to those of the fresh sample (Table 1). Coherence with a simple physical model was preferred to a more sophisticated fitting, to emphasise the qualitative and even quantitative adequacy of the adopted model. The lines in Figure 8 reveal the best fit for the 300°C spectra, obtained for $R_e=28.9$ and 13.8 $k\Omega$, respectively for one and two impregnation cycles. The quality of the fit is fairly good, considering that the model has a single variable. According to the present hypothesis, the R_e values may be used to obtain estimates of the p-type electronic conductivity by

$$\sigma_p = L/S.R_e^{-1}, \quad [2]$$

where L and S are the length and cross section area defining the volume available for transport. Estimates of σ_p obtained for different L/S values are shown in Figure 9: data set 1 assumes the thickness, L_p , and surface area, S_p , of the pellet; data set 2 is based on the same L , but on a restricted value $S_r = S_p(S_{tr/gr}/S_{gr})$, where $S_{tr/gr}$ is the effective area available for transport per grain (calculated from an average shell thickness of $1.5 \mu\text{m}$) and S_{gr} is the area of a grain assuming an equivalent grain diameter of $15 \mu\text{m}$; data set 3 assumes high σ_p surface regions with S_r and L restricted to $200 \mu\text{m}$ (impregnation to a $100 \mu\text{m}$ depth from both surfaces of the pellet) in series with a low σ_p bulk. In the absence of low temperature experimental data, the σ_p values taken for the undoped regions were obtained by extrapolation of the $\text{La}_{0.9}\text{Sr}_{0.1}\text{GaO}_{3-\delta}$ high temperature behaviour. It is important to note that substitution of Ga by Mg has practically no effect on σ_p . The latter set of values is in good agreement with the data obtained for homogeneous $\text{La}_{0.9}\text{Sr}_{0.1}\text{Ga}_{1-x}\text{Fe}_x\text{O}_{3-\delta}$ ($x=0$ and 0.2) by oxygen permeability measurements (9). The data show a clear Arrhenius-type behaviour with activation energy of about 75.1 kJ/mol . This value, obtained at low temperature ($300\text{-}375^\circ\text{C}$), is lower than that obtained for homogenous samples at $700\text{-}1000^\circ\text{C}$, ca. 88.8 kJ/mol for $x=0.2$ and 93.6 kJ/mol for $x=0$ (9). Such difference may be related to the fraction of tetravalent iron, which is expected to be higher at low temperature (20) thus facilitating the hopping of small polarons between Fe^{4+} and Fe^{3+} .

Ongoing work, to complete the electrochemical characterisation of the core-shell ceramics, namely by oxygen permeability measurements, is expected to confirm the present analysis.

4. FINAL REMARK

The present results show a remarkable effect on the transport properties of LSGM due to heterogeneous doping with Fe. The exact location of the electrically active Fe-rich areas (inside the grains, a typical core-shell microstructure, or outside the grains, as a secondary phase along the LSGM grain boundaries) still needs further confirmation. Both effects might even coexist under certain circumstances, with one prevailing over the other for specific processing conditions. What seems unquestionable is the use of a unique localized doping solution, taking advantage of the distinct grain boundary transport properties with respect to the grain bulk, to reach a new type of material, with heterogeneous distribution of one of the components (Fe), with major relevance on the total electrical transport properties. We describe this procedure as grain boundary engineering, and we believe that this is the first report on such an attempt to adjust the transport properties of oxygen ion conductors.

CONCLUSIONS

Core-shell ceramics with a $\text{La}_{0.95}\text{Sr}_{0.05}\text{Ga}_{0.90}\text{Mg}_{0.10}\text{O}_{3-\delta}$ core and a shell made of the same material doped with iron were obtained using a diffusion couple of $\text{La}_{0.95}\text{Sr}_{0.05}\text{Ga}_{0.90}\text{Mg}_{0.10}\text{O}_{3-\delta}$ and $\text{LaFeO}_{3-\delta}$. The diffusion of Fe into the gallate occurs preferentially along the grain boundaries

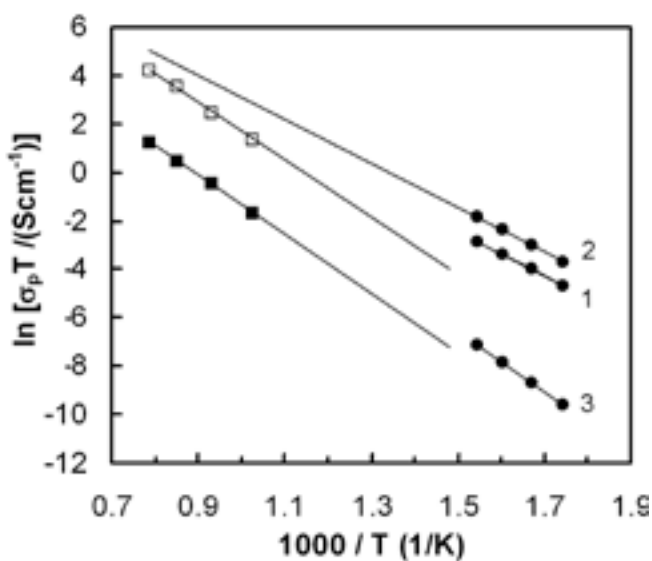


Fig. 9- Arrhenius representation of the electronic conduction parameter in air for one Fe-doped LSGM sample after the second impregnation cycle (solid circles): 1) pellet L/S , 2) S restrictions, 3) L and S restrictions (see text for details). The squared symbols correspond to data obtained for $\text{La}_{0.9}\text{Sr}_{0.1}\text{Ga}_{1-x}\text{Fe}_x\text{O}_{3-\delta}$ ($x=0$ - solid; $x=0.2$ - open) taken from ref. (9).

and a shell thickness of 1-2 μm was obtained upon annealing at 1550°C for three hours.

The study of these samples by impedance spectroscopy revealed that iron doping leads to an increase in p-type electronic conduction. An estimated value of 3.1×10^{-6} S/cm at 300°C in air for p-type electronic conductivity was obtained by fitting the low temperature impedance spectra to an equivalent circuit model. The activation energy was 75.1 kJ/mol between 300 and 400°C. These values are in good agreement with the expected trend observed for homogeneous ceramics but should be complemented by oxygen permeation measurements to confirm the potential of heterogeneous microstructures as mixed conducting materials.

ACKNOWLEDGEMENTS

This work was supported by FCT (project POCI/CTM/59727/2004), Portugal. Eduarda Gomes would like to thank PRODEP for funding (4/5.3/PRODEP/2000). Valuable comments of the referees are also acknowledged.

REFERENCES

- H.J.M. Bouwmeester, A.J. Burggraaf, Dense ceramic membranes for oxygen separation, in: A.J. Burggraaf, L. Cot (Eds.), *Fundamentals of Inorganic Membrane Science and Technology*, Elsevier, Amsterdam, 1996, pp. 435-528.
- Y. Teraoka, H.M.Y. Zhang, K. Okamoto and N. Yamazoe, Mixed Ionic-Electronic Conductivity of $\text{La}_{1-x}\text{Sr}_x\text{Co}_{1-y}\text{Fe}_y\text{O}_3$ Perovskite-Type Oxides, *Mat. Res. Bull.* 23 51-58 (1988)
- H. Iwahara, T. Esaka, T. Mangahara, Mixed conduction and oxygen permeation in the substituted oxides for CaTiO_3 , *J. Appl. Electrochem.* 18 173-177 (1988)
- J.R. Jurado, F.M. Figueiredo, B. Gharbage, J.R. Frade, Electrochemical Permeability of $\text{Sr}_{0.97}(\text{Ti,Fe})\text{O}_{3.58}$ Materials, *Solid State Ionics*, 118 89-97 (1999).
- B. Gharbage, F.M. Figueiredo, R.T. Baker, F.M.B. Marques, Electrochemical permeability of $\text{La}_{0.9}\text{Sr}_{0.1}\text{Ga}_{1-x}\text{Fe}_x\text{O}_{3.87}$ *Electrochimica Acta* 45 2095-2099 (2000)
- M. Feng, J.B. Goodenough, A superior oxide-ion electrolyte. *Eur. J. Solid State Inorg. Chem.* 31 663-672 (1994)
- T. Ishihara, H. Matsuda, Y. Takita, Doped LaGaO_3 perovskite type oxide as a new oxide ionic conductor, *J. Am. Chem. Soc.*, 116(9) 3801-3803 (1994)
- R.T. Baker, B. Gharbage, F.M.B. Marques, Ionic and Electronic Conduction in Fe and Cr Doped $(\text{La,Sr})\text{GaO}_{3.87}$, *J. Electrochem. Soc.* 144[9] 3130-3135 (1997)
- B. Gharbage, F.M. Figueiredo, R.T. Baker, F.M.B. Marques, Electrochemical permeability of $\text{La}_{0.9}\text{Sr}_{0.1}\text{Ga}_{1-x}\text{Fe}_x\text{O}_{3.87}$ *Electrochimica Acta* 45 2095-2099 (2000)
- K. Sasaki, H.P. Seifert, L.J. Gaukler, Electronic Conductivity of In_2O_3 Solid Solutions with ZrO_2 , *J. Electrochem. Soc.* 141(10) 2759-2768 (1994)
- V.V. Kharton, A.V. Kovalevsky, A.P. Viskup, F.M. Figueiredo, A.A. Yaremchenko, E.N. Naumovich and F.M.B. Marques, Oxygen Permeability of $\text{Ce}_{0.8}\text{Gd}_{0.2}\text{O}_{2.8} - \text{La}_{0.7}\text{Sr}_{0.3}\text{MnO}_{3.8}$ Composite Membranes, *J. Electrochem. Soc.* 147[7] 2814-2821 (2000)
- D. Hennings, G. Rosenstein, Temperature-Stable Dielectrics Based on Chemically Inhomogeneous BaTiO_3 , *J. Am. Ceram. Soc.* 67[4] 249-254 (1984)
- V. Pessey, D. Mateos, F. Weill, F. Cansell, J. Etourneau, B. Chevalier, SmCo_2/Cu Particles Elaboration Using a Supercritical Fluid Process, *J. of Alloys and Compounds* 323-324 412-416 (2001)
- T. Oku, T. Nakayama, M. Kuno, Y. Nozue, L.R. Wallenberg, K. Niihara, K. Suganuma, Formation and Photoluminescence of Ge and Si Nanoparticles Encapsulated in Oxide Layers, *Mat. Sci. and Eng B74* 242-247 (2000)
- F.M. Figueiredo, V.V. Kharton, J.C. Waerenborgh, A.P. Viskup, E.N. Naumovich, J.R. Frade, Influence of Microstructure on the Electrical Properties of Iron-Substituted Calcium Titanate Ceramics, *J. Am. Ceram. Soc.* 87[12] 2252-2261 (2004)
- A.L. Shaula, R.O. Fuentes, F.M. Figueiredo, V.V. Kharton, F.M.B. Marques, J.R. Frade, Grain size effects on oxygen permeation in submicrometric $\text{CaTi}_{0.8}\text{Fe}_{0.2}\text{O}_{3.8}$ ceramics obtained by mechanical activation, *J. Euro. Ceram. Soc.* 25 2613-2616 (2005)
- B. Boukamp, A Non-Linear Squares Fit Procedure Analysis of Imittance Data of Electrochemical Systems, *Solid State Ionics*, 20 31-44 (1986)
- E. Gomes, M.R. Soares, F.M. Figueiredo, F.M.B. Marques, Conductivity of $\text{La}_{0.95}\text{Sr}_{0.05}\text{Ga}_{0.90}\text{Mg}_{0.10}\text{O}_{3.8}$ obtained by mechanical activation, *J. Euro. Ceram. Soc.* 25 2599-2602 (2005)
- C. Haavik, E.M. Ottesen, K. Nomura, J.A. Kilner, T. Norby, Temperature dependence of oxygen ion transport in Sr+Mg-substituted LaGaO_3 (LSGM) with varying grain sizes, *Solid State Ionics* 174 233-243 (2004)
- F.M. Figueiredo, J. Waerenborgh, V.V. Kharton, H. Näfe, J.R. Frade, On the relationships between structure, oxygen stoichiometry and ionic conductivity of $\text{CaTi}_{1-x}\text{Fe}_x\text{O}_{3.8}$ ($x=0.05, 0.20, 0.40, 0.60$), *Solid State Ionics* 156 371-381 (2003)

Recibido: 15.07.05

Acceptado: 07.02.06

